sciendo

Environmental & Socio-economic Studies

DOI: 10.2478/environ-2026-0011

Environ. Socio.-econ. Stud., **2026, 14, 2: 24-37**

Original article

Geospatial analysis of the multidecadal and seasonal evolution of Sidi Rbat beach, Morocco, using GIS, topographic surveys, and digital elevation models

M'hamed Nmiss[1]*, Mahjoub Benbih[2], Hicham Irifi[3], Hassan Nait-Si[2], Abdelfattah Ben Kacem[3], Mhamed Amyay[3]

[1]Hassan II University of Casablanca, Faculty of Arts and humanities of Mohammedia, Laboratory of the Dynamics of Spaces and Societies (LADES), Mohammedia, Avenue Hassan II B.P. 546, Morocco
[2]Ibn Zohr University, Departement of Geography, FLSH Agadir, Agadir, BP 29/S 80000, Morocco
[3]Sidi Mohamed Ben Abdellah University, Faculty of Arts and Humanities Sciences Sais-Fez, Laboratory of Geo-Environmental Analyses and Sustainable Development – Planning (LAGEA-DD), Fès, BP 59 Route Imouzzer 30000, Morocco
*E–mail address (*corresponding author): mhamed.nmiss@usmba.ac.ma*
ORCID iD: M'hamed Nmiss: https://orcid.org/0009-0001-4107-3690; Mahjoub Benbih: https://orcid.org/0009-0008-5759-8097; Hicham Irifi: https://orcid.org/0000-0003-4323-060X; Hassan Nait-Si: https://orcid.org/0000-0003-3299-5447; Abdelfattah Ben Kacem: https://orcid.org/0009-0009-4112-904X; Mhamed Amyay: https://orcid.org/0009-0004-4207-3539

ABSTRACT

Sandy beaches are dynamic and vulnerable environments shaped by the interaction of hydrodynamic, fluvial, aeolian, and anthropogenic factors. This study presents the results of multi-decadal and seasonal monitoring of Sidi Rbat beach, located on the right bank of the River Massa on the Moroccan Atlantic coast. Two complementary approaches were applied. The first was a diachronic shoreline analysis over 53 years (1970–2023), based on aerial photographs and high-resolution satellite images, using the DSAS (Digital shoreline analysis system) tool within ArcGIS. The second approach consisted of the topographic monitoring of three beach profiles conducted between January 2019 and August 2021 using a total station. Two digital elevation models (DEMs), generated in summer (01/09/2020) and winter (27/02/2021), were used to produce a differential DEM to quantify sand volumes and identify erosion and deposition zones. The results showed a general erosional trend, punctuated by phases of accretion. This erosion was mainly driven by geomorphological factors including beach configuration, hydrodynamic conditions characterized by energetic Atlantic waves from the NNW, and anthropogenic influences, particularly the reduction of sediment supply following the construction of a dam in 1972. At the seasonal scale, the beach displays a classical morphodynamic cycle, with winter erosion and summer accretion, suggesting the presence of potential sediment sources such as coastal dunes, north-to-south longshore transport, and offshore sediment remobilization. DEM analysis further highlighted the strong influence of seasonal hydrodynamics on beach morphology. This study provides a solid scientific basis for understanding mesotidal beach morphodynamics along the Moroccan Atlantic coast and supports integrated coastal zone management.

KEY WORDS: beach morphodynamics, digital shoreline analysis system, Moroccan Atlantic coast, sediment budget, beach morphology

ARTICLE HISTORY: received 21 January 2026; received in revised form 2 May 2026; accepted 11 May 2026

1. Introduction

Sandy beaches are complex and dynamic natural environments, subject to the impact of numerous hydro-dynamic and anthropogenic factors that influence their evolution. They correspond to shorelines where waves and coastal currents deposit and transport sediments larger than mud in size (PASKOFF & CLUS-AUBY, 2007). Over the past decades, studies conducted on beaches have shown that the retreat

of sandy coasts is a global phenomenon (SALMAN ET AL., 2004; MORTON, 2004; GOPINATH ET AL., 2005; HAPKE ET AL., 2006; LUIJENDIJK ET AL., 2018). This retreat has intensified in recent times (BIRD, 2000; ZHANG ET AL., 2004; NICHOLLS & CAZENAVE, 2010; VOUSDOUKAS ET AL., 2020), especially due to sea level rise and various human interventions, such as the retention of terrigenous inputs by dams, the extraction of aggregates for construction purposes, the destruction of foredunes, and the depletion of nearshore sand stocks through dredging. An examination of research conducted along the Moroccan Atlantic coast shows that the general trend of beach evolution is one of shoreline regression (AOUICHE ET AL., 2016; BOURHILI ET AL., 2023; AANGRI ET AL., 2024; LHARTI ET AL., 2024). However, other studies have instead reported shoreline progradation or stability, particularly on beaches with limited human influence (NMISS ET AL., 2021a; NMISS ET AL., 2022; NMISS ET AL., 2025a). In reality, diagnosing whether a beach is in regression or progradation is a delicate task, as within a single sedimentary cell, there may be zones of erosion, stability, and accretion. Therefore, beach studies require temporal monitoring to understand the mechanisms driving their dynamics.

In recent years, the use of Geographic Information Systems (GIS) and Differential Digital Elevation Models (DEMs) has become increasingly common in monitoring beach dynamics at both decadal and seasonal scales (PARDO-PASCUAL ET AL., 2012; CASTELLE ET AL., 2017; VOUSDOUKAS ET AL., 2020; KILAR, 2023; NAJI ET AL., 2025; NMISS ET AL., 2025b). GIS, due to its ability to collect, centralize, store, manipulate, analyze, and display georeferenced data (CLARKE, 1986; NAIT-SI ET AL., 2021), proves particularly well-suited to environments where multiple interacting components must be assessed. Likewise, producing differential DEMs through seasonal topographic monitoring provides a highly precise and clear understanding of beach responses to seasonal energy variations. They enable the detection and quantification of topographic changes on beaches over time, including erosion, sediment accumulation, and shoreline displacement. By subtracting two DEMs obtained at different dates, it is possible to quantify sediment gains and losses across the beach, allowing for the calculation of sediment budgets and the identification of erosion and accretion zones.

This research aimed to study the dynamics and evolution of the sandy beach of Sidi Rbat, located on the right bank of the River Massa, at different spatial and temporal scales–long, medium, and short term (Fig. 1c). First, a diachronic analysis of shoreline change between 1970 and 2023 was carried out based on high-resolution spatial data from various sensors. This analysis also relied on GIS tools, particularly the DSAS (Digital Shoreline Analysis System) extension integrated into ArcGIS. This tool allows for the automated quantification of shoreline change and identification of prevailing trends. Secondly, the seasonal evolution of the studied beach was examined using topographic surveys conducted with a total station and field-based digital elevation models. Several objectives were set in this research: firstly, to assess the evolution of the shoreline over the past five decades; secondly, to understand the beach's morphological response to seasonal energy peaks during winter and summer; thirdly, to highlight the different factors responsible for beach evolution in a mesotidal context strongly exposed to energetic Atlantic waves; and finally, to determine the areas of erosion and sediment accumulation on Sidi Rbat beach.

2. Study area

This research focused on Sidi Rbat beach, located on the right bank of the River Massa, approximately 30 km south of the city of Agadir (30° N). It is a closed beach measuring 850 metres in length and about 80 meters in width (Fig. 1c). The beach is bordered by a dune resting against a cliff that forms the immediate hinterland (Fig. 2). To the north, it is bounded by a rocky coast topped by a ten-metre-high cliff overlooking the ocean, dating back to the Upper Soltanian (Fig. 2) (BARRADA, 1996).From a geological perspective, the study area is controlled by the structure of the Western Anti-Atlas. This structure extends at depth beneath the Chtouka and Tiznit plains, where the Precambrian basement, composed of highly contrasting lithological materials (quartzites, rhyolite, sandstone, conglomerate, and schist), governs the major geological features of the region (OLIVA, 1972; BARRADA, 1996). Since 1991, the beach has enjoyed full protection status as part of the Souss Massa National Park, an area of high ecological and environmental value in the Souss Massa region (Fig. 1b). This status offers protection against human interventions that alter the coastal landscape, unlike the more urbanized beaches to the north such as Agadir, Anza, Taghazout, and Aghroud (AOUICHE ET AL., 2016; AANGRI ET AL., 2023).

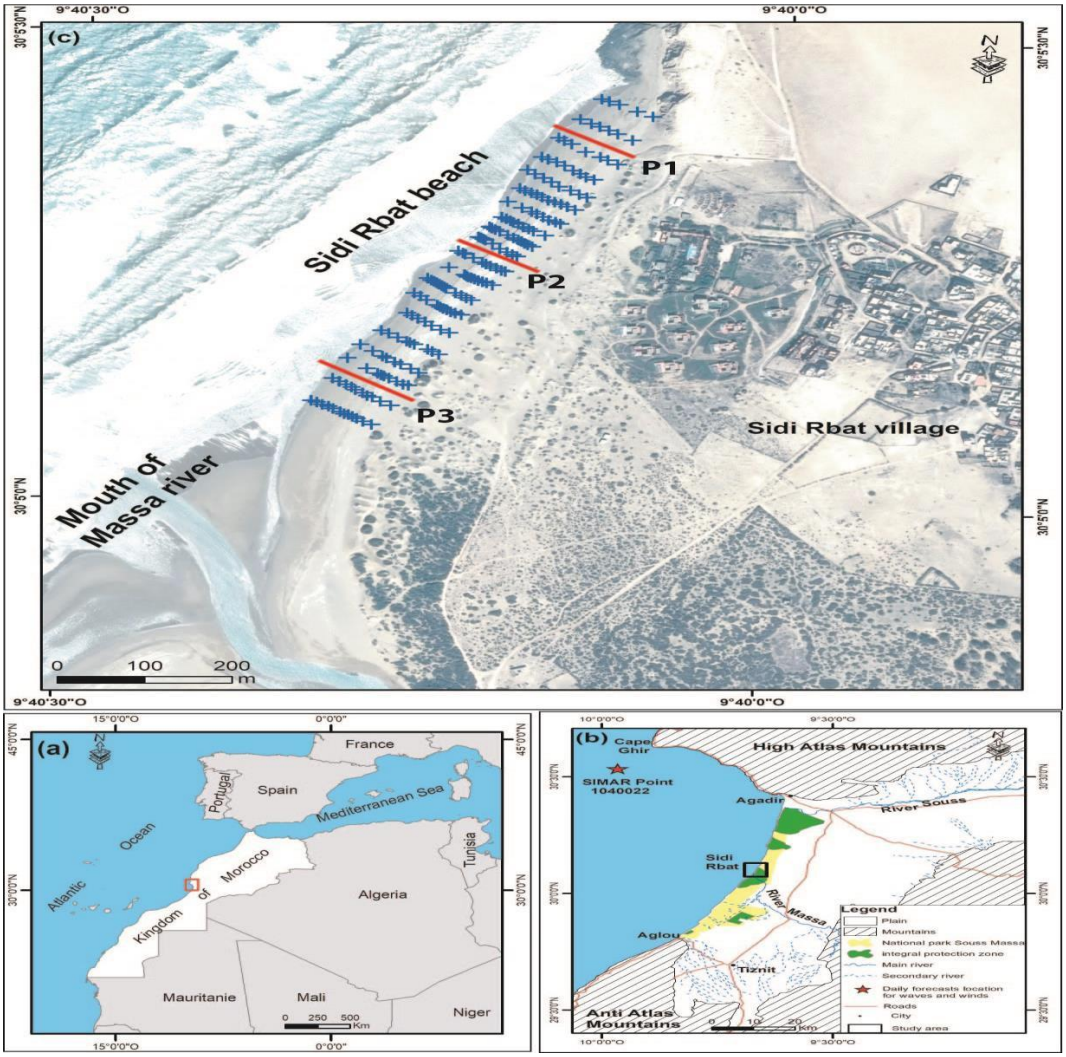

Fig. 1. Location of the study area: (a) Overview of the study site's position on the map of Morocco; (b) Location of Sidi Rbat beach within the territory of the Souss Massa National Park; (c) Location of the surveyed topographic profiles and points used to generate the Digital Elevation Models (DEMs), overlaid on a 2018 Pléiades satellite orthophoto

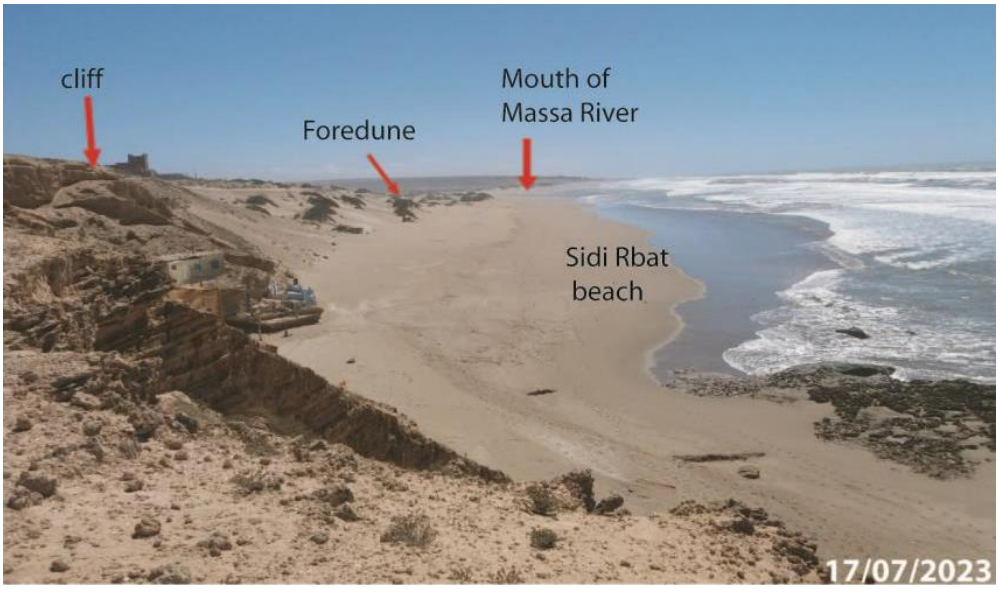

Fig. 2. A panoramic view of Sidi Rbat beach on the right bank of the River Massa

From a hydrodynamic perspective, Sidi Rbat Beach has a general NNE–SSW orientation and is highly exposed to energetic Atlantic waves from the NNW sector (NMISS ET AL., 2025b). Based on daily wave forecasts provided by Spanish port authorities at SIMAR point 1040022 (coordinates 30.500 N, -10.000 E) (Fig. 1b), 82.5% of the significant wave heights are below 2.5 meters, while 17.5% exceed this height (Fig. 3aI and 3aII). As for wave periods, 47.14% of the waves last longer than 10 seconds (Fig. 3bI and 3bII). This wave pattern indicates a predominantly swell-dominated regime in winter, and a mix of fair-weather swell and shorter-period waves in summer (NMISS, 2023). Dominant wave conditions originating from the north and north–northwest sectors induce a north–south longshore sediment drift, facilitating the southward transport of sands, particularly in the absence of any rocky headland likely to impede this process. The magnitude of longshore sediment transport within this littoral cell has been estimated at approximately 400,000 m^3/year (LCHF, 1972). Climatically, the study area is characterized by a Mediterranean-type climate, marked by an alternation between a hot, dry season and a mild, wet season. The average annual rainfall recorded at the nearest station, Melk Zhar (11 km from the coast), is 163 mm. This rainfall is marked by strong intra- and inter-annual variability. The average annual temperature is 21.53°C. Dominant winds in this coastal sector blow mainly from the northwest (82%), followed by the southeast (14%) and the west (4%) (ATIKI ET AL., 2021) (Fig. 3c).

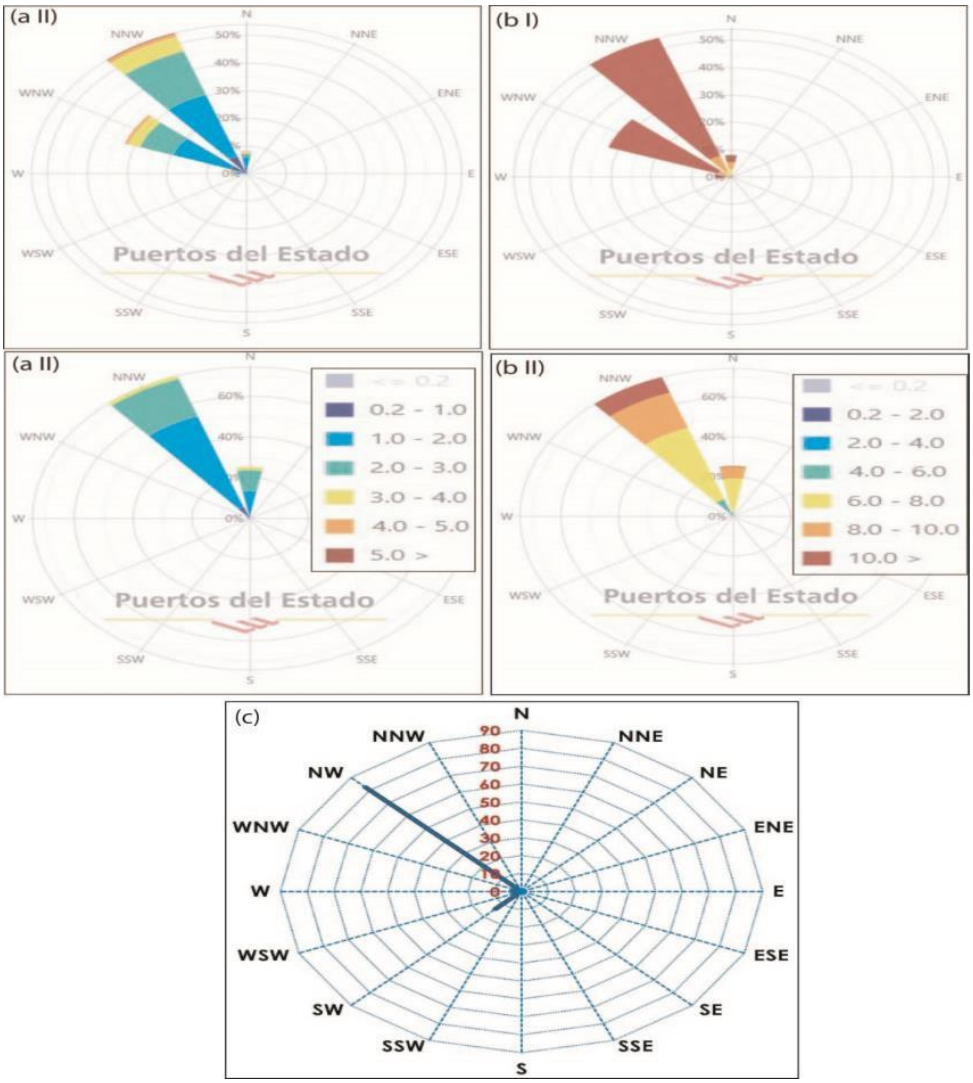

Fig. 3. Dominant hydrodynamic and wind conditions in the studied coastal area (aI) and (aII) Significant wave height during the winter (aI) and summer (aII) seasons. (bI) and (bII) Significant wave period in winter and summer (period: 1958–2021) (Source: SIMAR Point 1040022 (Fig 1 b); PORTUS database, available at https://portus.puertos.es). (c) Dominant wind direction and frequency at the Melk Zhar station (period: 1986–2020) (Source: Agadir Hydraulic Basin Agency)

3. Methods

The methodological approach adopted in this research aimed, to study the evolutionary trends of Sidi Rbat beach over the past half-century (1970–2023) and to conduct seasonal monitoring through Digital Elevation Models (DEMs) between 2020 and 2021.

3.1. Multi-decadal evolution of the shoreline (1970–2023)

To analyze the evolutionary trends of Sidi Rbat beach, we relied on photo-interpretation and Geographic Information Systems (GIS), which currently provide the best means to assess the evolutionary state of a beach at a given time. This study was based on high-resolution spatial data such as aerial photographs from two missions (1970 and 1986), satellite images from Google Earth Pro, and Pléiades satellite images (Table 1). Although these data reflect isolated and spontaneous situations, their comparison mainly allows highlighting the different stages of the geomorphological evolution of the coastline (NMISS ET AL., 2022; NAJI ET AL., 2025). The various spatial sources used were analyzed and processed through digital image processing methods. This approach is inspired by the work of THEILER & DANFORTH (1994) and includes several key steps, notably the geo-referencing of satellite images, correction of distortions and geometric transformations, digitization of shoreline lines, as well as diachronic overlay of the shorelines to study their temporal evolution. The georeferencing of satellite images was carried out using high-resolution orthophotos from the Pléiades satellite, aiming to minimize distortions and deformations that could affect diachronic analysis. Subsequently, the mean high water line was selected as the reference due to its good visibility on satellite images, particularly thanks to the contrast provided by the coloration of the exposed intertidal zone at low tide (ROBIN, 2005; CROWELL ET AL., 1991). This line is indeed one of the most frequently used indicators to analyze shoreline variations (DOLAN ET AL., 1983; MOORE, 2000; ARMAROLI ET AL. 2004; BOAK & TURNER, 2005; MOORE, 2006).

Table 1. Spatial data used for shoreline monitoring

Spatial data	Date of shoreline extraction	Scale (aerial photos) and resolution (satellite images)	Season period	Source
Aerial photography	November 14, 1970	1/ 30000	Autumn	National Agency of Land Conservation Cadastre and Cartography, technical documentation service
	March 22, 1986	1/ 20000	Intermediate (Hiver Spring)	
Satelitte images	March 28,2023	1 m	Spring	Google Earth Pro
	October 24, 2020		Autumn	
Pleiades orthophotography	October 29, 2018	0.5 m	Autumn	Cartographic Department of the Urban Agency of Agadir
Orbview 3	November 21, 2005	1 m	Autumn	https://earthexplorer.usgs.gov/

To measure the geomorphological evolution of the shoreline at the beaches of Sidi Rbat and Tifnit, we used version 5 of the Digital Shoreline Analysis System DSAS, a software extension developed by the U.S. Geological Survey (USGS) (HIMMELSTOSS ET AL., 2018) and integrated into the ArcGIS 10.5 environment. Developed to analyze historical coastal dynamics based on dated shorelines, this tool allows calculation of change rates from diachronic data (THEILER & DANFORTH, 1994; TEMITOPE & OYEDOTUN, 2014). More specifically, DSAS provides statistics on shoreline variations relying on a time series of coastline lines. The tool operates by generating transects perpendicular to a hypothetical reference line called the "baseline," positioned parallel to the shore. The intersection of these transects with different shoreline positions enables the calculation of two main indicators. The first, the Net Shoreline Movement (NSM), measures the distance between the oldest and most recent shoreline lines for each transect. The second, the End Point Rate (EPR), corresponds to the rate of shoreline displacement, obtained by dividing this distance by the time interval between the two extreme dates. The choice of EPR was motivated by the temporal structure of the available shoreline dataset, characterized by irregular acquisition intervals and a limited number of shoreline positions for certain sectors, conditions under which EPR remains one of the most suitable and widely used indicators for long-term coastal

change assessment. Although other DSAS metrics such as Linear Regression Rate (LRR), Weighted Linear Regression (WLR), and Shoreline Change Envelope (SCE) can provide additional information on temporal variability and statistical trends, their application generally requires a denser and more continuous chronological series of shoreline data. Consequently, EPR and NSM were considered the most appropriate indicators for ensuring methodological consistency and comparability across the study area.

Methodologically, it is essential to consider the various sources of uncertainty that may influence the results of the diachronic shoreline analysis. These uncertainties relate notably to the quality of the aerial photographs and satellite images used, the accuracy of georeferencing, shoreline extraction, default parameters used by the DSAS tool, as well as tidal effects and seasonal conditions at the time of image acquisition (Appeaning Addo et al., 2008; Jonah et al., 2016). Because the shoreline dataset spans a long temporal range (1970–2023), the quality and spatial resolution of the imagery vary considerably between historical aerial photographs and recent high-resolution satellite images. Consequently, uncertainty values were not considered uniform for all datasets but were evaluated according to the characteristics of each image source. Older aerial photographs, characterized by lower spatial resolution and greater geometric distortion, were associated with higher positional uncertainties than recent orthorectified satellite images. The uncertainty related to image quality was estimated based on image resolution, visual

interpretation conditions, and orthorectification precision, with an average uncertainty of ±0.6 m for recent images and higher values assigned to older photographs where necessary. Georeferencing uncertainty was assessed using the Root Mean Square Error (RMSE) obtained during the rectification process, averaging ±1.7 m. Regarding shoreline extraction, an uncertainty of ±2.5 m was retained, determined based on successive repetitions of manual digitization of the shoreline. As for the default data integrated into DSAS, the U.S. Geological Survey (USGS) recommends a standard uncertainty of 10 m. This value represents an approximate average derived from different types of shoreline data used in recent regional reports within the framework of the National Assessment of Shoreline Change program (Himmelstoss et al., 2018). Finally, the variation due to tidal state was evaluated at +58.86 m, based on the coastal profile slope (θ) and water height (h), according to the formula: $\Delta d = h/\tan(\theta)$ (Thomas & Diaw, 1997).

To analyze shoreline evolution using the mean high water line as a reference, it is essential to assess the uncertainty related to tidal variations (between high tide and low tide). Stafford & Langfelder (1971) emphasized the importance of minimizing the effects induced by these variations in comparative studies based on photo-interpretation and satellite data. According to them, images must be acquired synchronously and under similar tidal conditions to ensure the reliability of results. In this study, tidal conditions at the time of each image acquisition were obtained from data recorded at the port of Agadir. This data were obtained from the French Hydrographic and Oceanographic Service database, available at https://www.shom.fr. Furthermore, the beach slope at the time of aerial photography and satellite image acquisition is a key parameter for estimating the error margin induced by tides. However, precise data regarding the slopes of the studied beaches at the time of image acquisition are not available. To address this gap, we used the average slopes derived from topographic profiles measured between 2019 and 2021. Based on these slopes (θ) and water heights (h), the difference between extreme mean sea levels can be estimated using the formula proposed by Thomas & Diaw (1997): $\Delta d = h/\tan(\theta)$. The tidal variation was evaluated at +58.86 m.

The estimation of the total uncertainty (UT) is based on calculating the square root of the sum of the squares of the individual error sources (Taylor, 1997). Considering inaccuracies related to data quality (± 0.6 m), georeferencing (RMS) (± 1.7 m), shoreline identification (± 2.5 m), the standard uncertainty of the DSAS module (± 10 m), as well as the variability of the reference line position (mean high water line) (± 58.86 m), the overall estimated error for the period 1970–2023 is approximately ± 8.86 m. This value corresponds to an average annual uncertainty of ± 0.16 m/year.

3.2. Seasonal evolution of beaches

In order to characterize the seasonal evolution of the Sidi Rbat beach, we conducted a topographic survey of the intertidal and supratidal zones of the beach over a three-year period (2019–2021). This monitoring was carried out using a high-resolution SOUTH NTS-375R electronic total station (with an accuracy of approximately ±1.5 mm, according to

the manufacturer's specifications) (Figs. 4a and b). The operation of this station is based on sighting a reflective target, held by an operator positioned at the measurement point (NMISS ET AL., 2025a). In total, three topographic profiles were established. These profiles were surveyed perpendicular to the shoreline from January 2019 to August 2021. Five measurement campaigns were conducted according to a winter/summer schedule. The selection of these two seasons for the topographic surveys aimed to observe how these complex environments respond to energy extremes, which are particularly marked in winter and summer, as opposed to the transitional seasons (autumn and spring). Another objective was to study the annual morphological cycle of the surveyed beaches.

Fig. 4. Topographic survey instrument(a) Setup of the SOUTH NTS-375R electronic total station. (b) The rod and reflective target used for the survey

To calculate the sediment budget along the different profiles, we used the Profiler 3.1 software developed by (COHEN., 2014). This software, integrated as an add-in within Microsoft Excel (Office 2010), is notable for its accessibility and ease of use. It calculates sediment volume based on topographic profiles by establishing a relationship between cumulative distance and profile elevation. Although other tools exist for assessing volumetric changes, such as BMAP (Beach Morphology Analysis Package), BPAT (Beach Profile Analysis Toolbox), or certain AutoCAD modules like Covadis, these alternatives often involve greater complexity or higher acquisition costs.

In order to characterize the seasonal morpho-dynamics of Sidi Rbat beach, we also developed two digital elevation models (DEMs) to highlight the morphological variations between winter and summer. These two models were created in September 2020 (01/09/2020) and January 2021 (27/02/2021). The generation of a differential DEM also enabled us to identify zones of sediment accumulation and erosion, as well as to calculate the volume of sand mobilized on the beach. The method involves surveying as many measurement points as possible across the entire beach, focusing on areas where apparent morphological changes occur. A total of 177 points were surveyed across the Sidi Rbat beach (Fig 1c). In order to ensure the comparability of the two DEMs, the measurements were carried out along the same survey transects and, as far as possible, at identical or very close spatial positions using GPS positioning.

The collected elevation data were processed using Surfer 10 (GOLDEN SOFTWARE, 2010), which allows interpolation of irregularly distributed topographic datasets (JABBAR, 2016). The DEMs were generated using the kriging interpolation method, selected for its ability to provide smooth surface reconstruction and minimize interpolation errors in coastal topographic studies. A spherical variogram model was applied after testing several theoretical models. The variogram parameters were adjusted according to the spatial structure of the measured data, considering the range, sill, and nugget effects in order to optimize interpolation performance. The resulting DEMs were produced with a spatial resolution of 1 m. Prior to interpolation, the elevation datasets were checked for outliers and inconsistencies, and minor smoothing was applied to reduce local noise while preserving the main geomorphological features of the beach surface.

The comparison between the two survey campaigns (September 2020; February 2021) was then used to generate a differential DEM, allowing the quantification of seasonal elevation changes and sediment volume variations between the winter and summer periods. In this analysis, the DEM generated from the first survey campaign

(September 2020) was used as the reference surface (baseline), while the DEM derived from the second campaign (February 2021) represented the comparison surface. Sediment volume changes were calculated by subtracting the elevation values of the reference DEM from those of the second DEM on a cell-by-cell basis. Positive values indicate sediment accumulation, whereas negative values correspond to erosion zones. No uniform planar surface was assumed in the calculations, as the analysis relied entirely on the comparison between the two measured topographic surfaces.

4. Results

4.1. Multi-decadal evolution of the shoreline

Monitoring the shoreline of Sidi Rbat beach on the right bank provides insights into its dynamics over a timescale of more than half a century (1970 to 2023). The processing and analysis of various spatial data sources (aerial photographs, satellite images) made it possible to reveal the beach's evolutionary trends and to identify areas of erosion, accretion, and relative stability. The results of the diachronic study show a complex evolution, with a clear dichotomy between the north (long-term erosive) and the south (long-term accretional, especially in recent years). The recent period (since 2018) is marked by a nearly generalized accretion phase, reversing previous trends in certain sectors. Over the long term (1970–2023), Sidi Rbat beach shows a strong contrast between its northern and southern parts (Fig. 5). On one hand, the northern and central sectors show significant net erosion. The retreat rate in this area varies from -1.18 m to -66.47 m, corresponding approximately to transects 1 to 661 (Fig. 5). On the other hand, the southern sector– located directly on the right bank of the River Massa–exhibits a marked net accretion, with shoreline advance ranging from +0.89 m up to +120.10 m (transects 661 to 852). For the 1970 – 1986 period, the observed pattern is similar to that of the full 1970–2023 period, with erosion clearly dominating across almost the entire northern and central parts of the beach (Fig. 5). The highest rate of shoreline retreat is recorded in the central part of the beach at -55.42 m, or about -3.46 m/year. During the 1986–2005 period, the shoreline continued to show an overall erosive trend, although the intensity of erosion appears slightly lower in some sectors compared to earlier periods (Fig. 5). A few very localized zones of accretion appear in the southern sector, with a maximum advance of 14 m (approximately +0.66 m/year), but these remain minor. However, starting from the 2005–2018 period, the general shoreline trend began to reverse spatially (Fig. 5). The northern and central sectors (approximately transects 1 to 613) now show a trend toward stability or even slight accretion. In contrast, the southern sector (approximately transects 613 to 865) continues to experience significant erosion. On a much shorter timescale of five years (2018–2023), a notable shift in shoreline dynamics is observed (Fig. 5). Accretion has become the dominant trend across nearly the entire beach. It is particularly pronounced in the southern sector, reversing the erosive trend observed in that area during the 2005–2018 period. A very slight erosion persists only at the northernmost tip of the beach (first transects).

4.2. Seasonal evolution of the beach

The topomorphological monitoring of three shore-perpendicular profiles over a three-year period (2019–2021) made it possible to reveal the morphological response of Sidi Rbat beach to winter and summer energy extremes. Three topographic profiles were surveyed along this beach (Fig. 1c). The first and second profiles are located at the northern end and the centre of the beach, respectively, while the third profile is situated at the southern end (Fig. 1c). To simplify the presentation of results, the different surveyed profiles are summarized in Figure 6 below. Across all the profiles, the results show a classic (normal) morphological cycle with erosion during the winter season and accretion during the summer season (Fig. 6). In detail, Profiles 1 and 2 display an irregular to convex shape in the foreshore and upper beach. The average slope of these two profiles is 6.22 for Profile 1 and 3.2 for Profile 2. The volumetric changes recorded between September 2019 and February 2020 indicate erosion rates of -0.4 m^3/m (P1) and -0.6 m^3/m (P2) (Fig. 7). During the summer, a significant accretion is observed in the intertidal zone, with the formation of a littoral bar and a small scarp (micro-cliff) in the mid-foreshore area. The summer sediment budget between February 2020 and July 2020 is about +0.7 m^3/m in Profile 1 and +0.8 m^3/m in Profile 2 (Fig. 7). In contrast, the third profile exhibits an irregular concave–convex shape, with an average slope of 1.44. The winter hydro-dynamic variations result in a relatively smooth profile,

especially in the intertidal zone (Fig. 6). However, irregularities are observed in the other parts of the beach profile, mainly due to a sand berm located at the foredune. The volumetric variations show a sediment budget of -0.1 m^3/m in winter and +0.2 m^3/m in summer (Fig. 7).

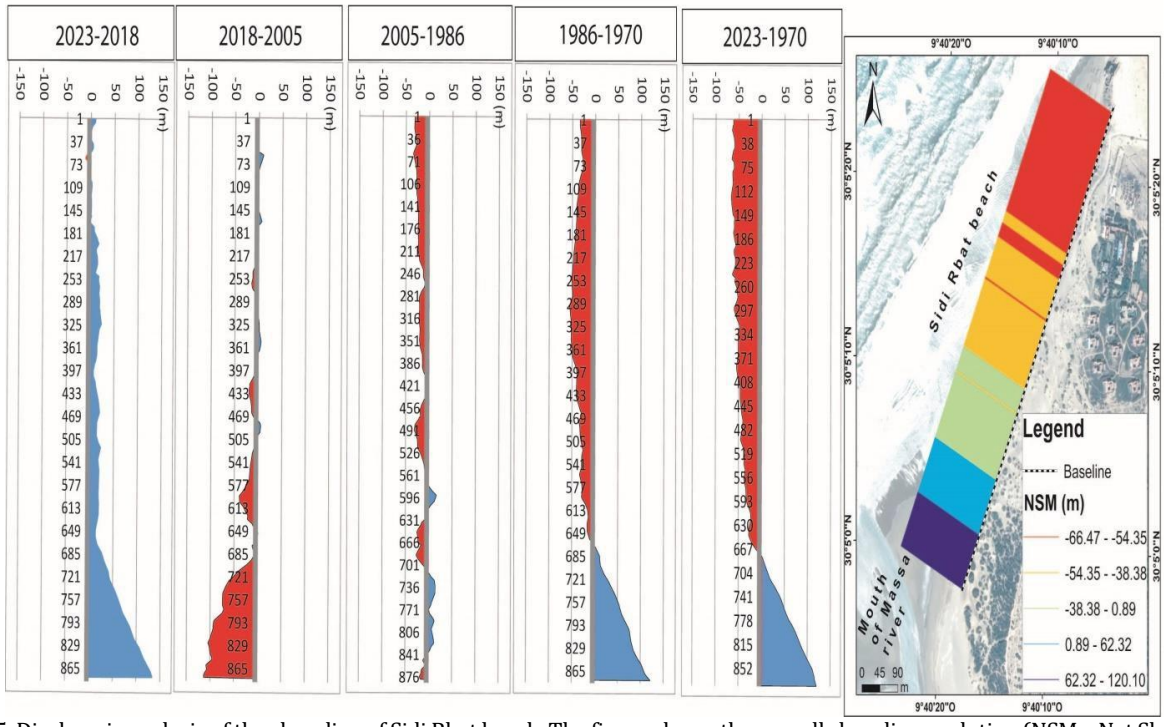

Fig. 5. Diachronic analysis of the shoreline of Sidi Rbat beach. The figure shows the overall shoreline evolution (NSM – Net Shoreline Movement) for the period 1970–2023, as well as for specific time intervals: (1970–1986), (1986–2005), (2005–2018), and (2018–2023)

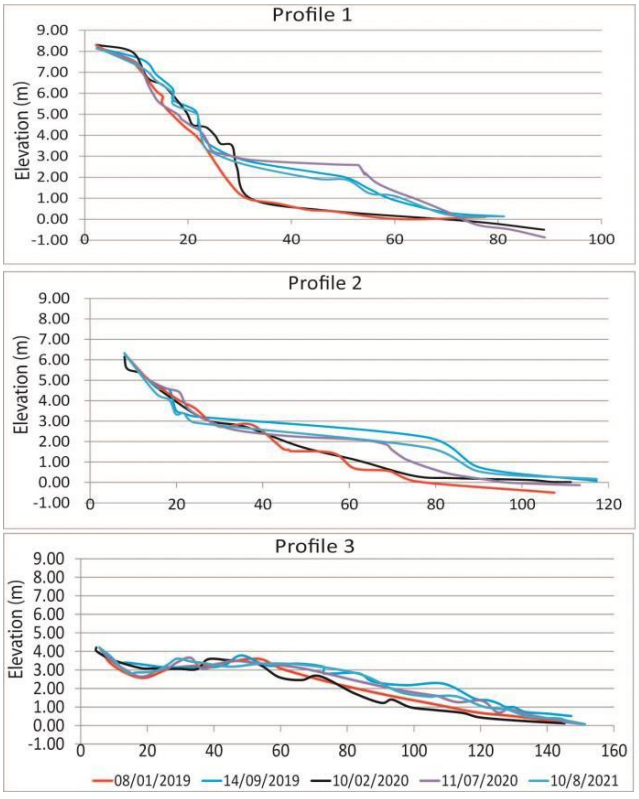

Fig. 6. Morphological evolution of the three surveyed profiles on Sidi Rbat beach over five survey campaigns

To characterize the morphodynamics of Sidi Rbat beach and calculate the volume of sediments displaced, we also produced two DEMs and a differential DEM. The goal here was to reveal how Sidi Rbat beach responds to seasonal energy extremes. During the first field campaign (01/09/2020), the results suggest a relatively nourished beach, typical of a summer period when calmer swell conditions may have favoured sediment accumulation (Figs 8 and 9a). The calculated sand volume during this period was 45,996.69 m^3 (Fig. 8). During this time, Sidi Rbat beach was well supplied with sediments, with rocky outcrops in the intertidal zone covered by sand (Fig. 9a). In contrast, during the second field campaign (27/02/2021), the dominant feature was beach erosion, reflecting the strong energy of the winter waves (Figs. 8 and 9b). The calculated sand volume at this time was 32,483.34 m^3 (Fig. 8). This decrease in sand volume demonstrates the influence of winter hydrodynamics on Sidi Rbat beach. In the field, rocky outcrops appeared at the surface, increasing wave energy and turbulence (Fig. 9b). Micro-cliffs were also formed at the foredune area at the upper beach (Fig. 9b). The creation of a differential DEM enabled us to calculate the volume

of sand displaced on one hand and to identify erosion and accumulation zones on the other. In total, 13,513.35 m^3 of sediment were mobilized on the beach between the summer and winter seasons (Fig. 9). Figure 10 of the differential DEM highlights dominant and significant erosion over the entire beach.

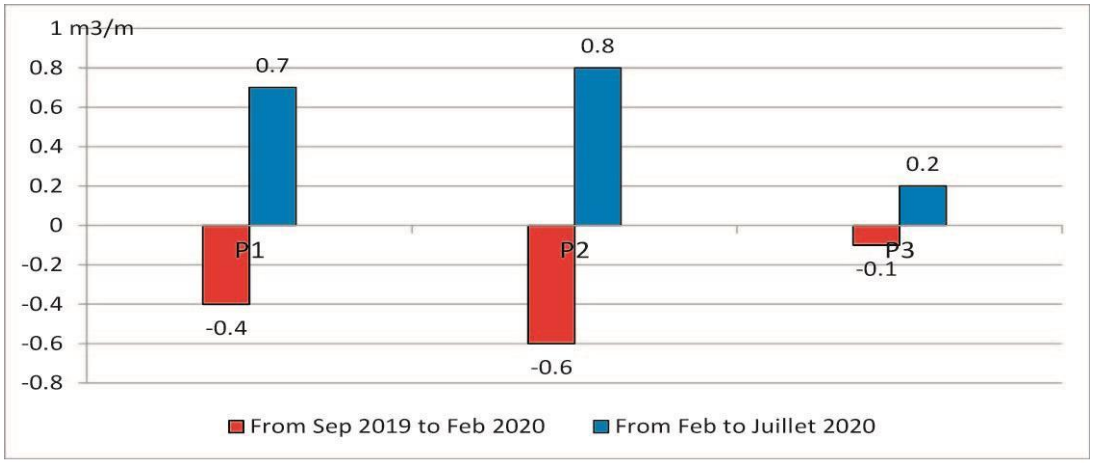

Fig. 7. Sediment budget recorded over a one-year period

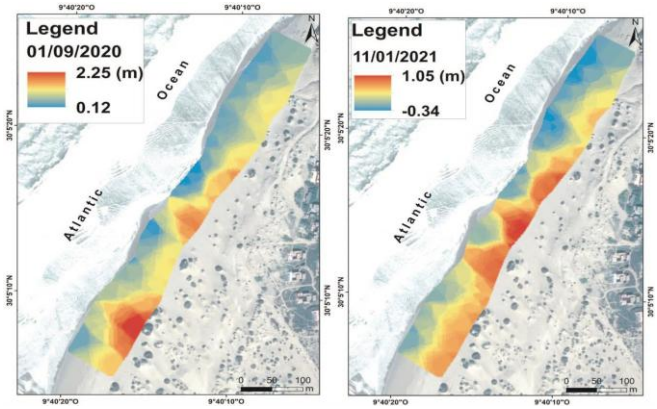

Fig. 8. Digital Elevation Models (DEMs) obtained during two field campaigns (summer 2020 and winter 2021)

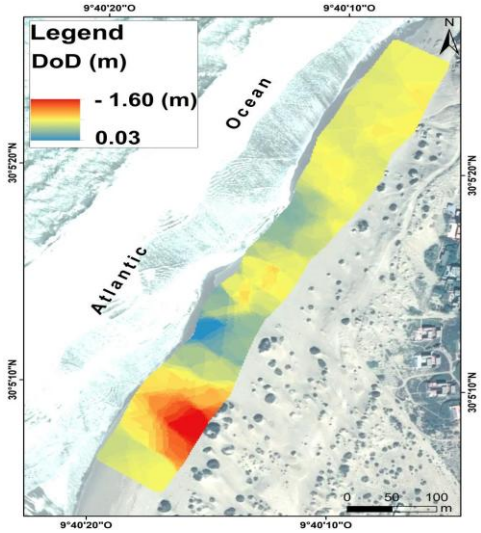

Fig. 9. DoD represents the Differential DEM

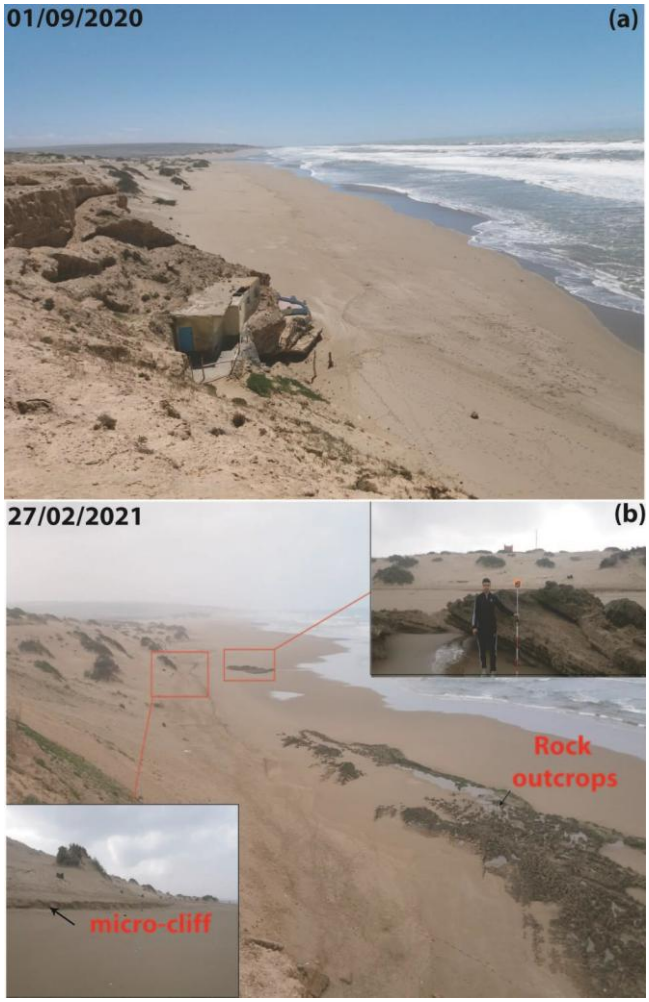

Fig. 10. Impact of seasonal hydrodynamics on the morphology of Sidi Rbat beach. Images 1 and 2 were taken during topographic surveys for creating the DEMs

5. Discussion

5.1. An evolutionary trend toward erosion

The diachronic analysis of the shoreline of Sidi Rbat beach on the right bank of the River Massa, using high-resolution spatial data and GIS tools, revealed the evolutionary trend of the beach over a 53-year period (1970–2023). The results indicate a general trend toward erosion, although some accumulation zones persist. This erosion can be explained by several factors. First, Sidi Rbat beach is a pocket beach backed by a cliff. This morphological configuration significantly contributes to erosion and shoreline retreat. Cliffs, by their morphodynamic nature, are inherently erodible systems that enhance wave energy reflection (CARTER, 1988; NAYLOR ET AL., 2010; KENNEDY ET AL., 2014). When waves reach Sidi Rbat beach, part of their energy is absorbed by the sand and other beach components. However, in the presence of a cliff, this energy is reflected back offshore, causing increased turbulence and more significant erosion. Second, Sidi Rbat beach is subjected to strong marine hydrodynamics, reflected in a steeper foreshore slope (MANSOUM, 1994; NMISS, 2023). This morphological characteristic offers no protection against powerful waves coming from the NNW sector. It reduces the beach's capacity to dissipate wave energy, making it more vulnerable to wave and storm impacts. A steep foreshore slope means that waves reach the coast with higher kinetic energy, causing greater beach erosion. Third, the construction of the Youssef ibn Tachafine dam upstream on the Massa River has had a significant impact on the sediment supply to the Massa beaches. By retaining 17 million cubic meters of sediment, the dam has considerably reduced the amount of sediment available for the renewal of Sidi Rbat beach (NMISS ET AL., 2025b). This reduction in sediment supply has multiple consequences for the long-term evolution of the shoreline. Without sufficient sediment input, Sidi Rbat beach is more prone to accelerated erosion because it cannot naturally regenerate at a rate sufficient to compensate for losses due to wave and current action. Fourth, the strong north-to-south littoral drift plays a major role in the shoreline evolution and erosion of Sidi Rbat beach. It can cause sediment stock displacement from the beach toward the south, creating a cumulative effect at the mouth of the River Massa to the south (NMISS ET AL., 2022).

This pattern of short-term morphodynamic variability is consistent with observations made in other high-energy coastal environments. For instance, UŚCINOWICZ ET AL. (2025) documented similar rapid shoreline adjustments along the Baltic Sea coast, highlighting the role of energetic hydrodynamic forcing and sediment redistribution in controlling short-term coastal evolution. Their results, based on comparable GIS and high-resolution spatial analysis methods, reinforce the interpretation that even in systems characterized by long-term erosion, short-term morphodynamic equilibria may occur under specific hydrodynamic conditions.

5.2. A classical seasonal morphological cycle

Seasonal topographic monitoring of Sidi Rbat beach reveals a classical morphological cycle, characterized by erosion during the winter seasons and sediment accumulation during the summer. Indeed, the beach's ability to restore the sediment stock lost during the winter raises important questions about potential sediment sources that could replenish the beach in the case of sediment shortage. During winter periods, high-energy meteo-marine conditions are frequently observed, with stronger waves. This is reflected not only in the topographic profile shapes but especially in volumetric changes (losses). As a result, rip currents carry large quantities of sediment offshore (FOX & DAVIS, 1978). These sediments are stored lower on the profile in the form of offshore sandbars. Thus, the overall trend observed across all winter profiles is one of erosion.

In contrast, during calmer hydrodynamic conditions in summer, waves are less powerful, which facilitates the onshore migration of sediments stored on offshore bars to the upper parts of the beach, leading to its thickening (DARLING, 1964; FOX AND DAVIS, 1978; AAGAARD ET AL., 2002; MASSELINK ET AL., 2008). This summer situation promotes beach accretion, with the formation of littoral bars on the foreshore and upper beach, as well as the development of sand berms at the base of the foredune (CASTELLE ET AL., 2007). The progradation of this dune system results from the combined action of marine and aeolian processes. The sediment availability initially stems from a marine sand accumulation that exceeds export rates, leading to beach nourishment (TELKIN, 2004; HOUSER, 2009). The formation of foredunes coincides with the aeolian transport of beach-deposited sediments. Depending on its transport capacity, wind

moves across the beach, mobilizing sand that is trapped by vegetation or topographic obstacles (consolidated dunes) (DELGADO-FERNANDEZ, 2011; HESP, 2013).

Unlike the long-term trend of coastal retreat, the short-term seasonal evolution of Sidi Rbat beach shows a morphodynamic equilibrium over a three-year period (2019–2021). This apparent stability results from the interaction of multiple feedback mechanisms that may enable the beach to compensate for sediment losses, especially during the summer. Indeed, Sidi Rbat beach's capacity to restore its sediment stock raises questions about the origin of this sediment, particularly in the context of reduced terrigenous inputs. The interpretation of this behaviour must therefore consider the influence of the River Massa, located immediately adjacent to the study area, which may constitute a potential sediment source or, conversely, a sediment-starved system due to upstream regulation and dam construction. We propose two hypotheses that may explain the beach's medium-term stability: The first hypothesis involves a new sediment supply source originating from offshore. This hypothesis is supported by several studies in similar high-energy coastal systems where offshore sand reservoirs act as buffers feeding the beach during calm conditions (e.g., AAGAARD ET AL., 2002; POATE ET AL., 2014), although its persistence under reduced fluvial input remains uncertain. The second hypothesis attributes the beach accretion to various morpho-sedimentary exchanges between the beach and foredunes, as well as to significant longshore sediment transport from the north (littoral drift), contributing to the beach's equilibrium. Such longshore transport-driven equilibrium has been widely documented in wave-dominated coasts, where sediment redistribution rather than external inputs controls beach stability (e.g., CASTELLE ET AL., 2007; VOUSDOUKAS ET AL., 2012).

Moreover, the production of Digital Elevation Models (DEMs) and a Differential DEM (DoD) enabled us to identify the transitional period from typically calmer summer conditions to more energetic winter conditions characterized by storms and high wave activity. On most beaches worldwide, winter storms are the main drivers of coastal erosion (MASSELINK ET AL., 2016; VOUSDOUKAS ET AL., 2012). Analysis of the DEMs and DoD highlights a strong erosive dynamic at Sidi Rbat beach between September 2020 and February 2021. This erosion resulted in a general thinning of the entire beach, including both intertidal and supratidal zones. Such erosion confirms that Sidi Rbat beach is subjected to intense marine hydrodynamic activity, reflected in its steep foreshore slope.

6. Conclusions

The study of the morphological evolution of Sidi Rbat beach, located on the right bank of the River Massa, through photo-interpretation and topographic monitoring, has revealed the beach's dynamics across different temporal scales – long, medium, and short term. Over the long term, the dominant trend is one of erosion, although certain periods of accretion and stability were observed. The causes of beach narrowing are manifold. They are primarily linked to the site's morphological configuration, its exposure to high-energy waves from the NNW sector, the strong north-to-south littoral drift that transports sediment stock southward, and the reduction of terrigenous inputs from the River Massa due to the upstream construction of the Youssef Ibn Tachafine dam, which traps a significant volume of sediment. In contrast, at the medium term, morpho-topographic monitoring of the intertidal and supratidal zones indicates a relatively balanced morphodynamic state, marked by a classical seasonal cycle (winter erosion/summer accretion). This apparent stability suggests the presence of potential sediment sources maintaining this equilibrium – primarily from the upper beach dune, which acts as a buffer against winter wave action. Part of the sediment also originates offshore and is supplemented by north-to-south longshore transport within the Souss-Massa coastal cell. In the short term, the analysis of two Digital Elevation Models and their differential shows significant erosion of the beach between September 2020 and February 2021. This episodic observation highlights the vulnerability of Sidi Rbat beach to erosion. A longer-term monitoring effort is required to determine whether this trend is persistent, cyclical, or indicative of a structural erosion process linked to site morphology. This study provides a useful foundation for planners and decision-makers aiming to develop an appropriate strategy for integrated coastal zone management, especially in the context of global climate change and sea-level rise.

References

Aagaard T., Black K.P., Greenwood B. 2002. Cross-shore suspended sediment transport in the surf zone: A field-based parameterization. *Marine Geology,* 185, 3–4: 283–302.

Aangri A., Hakkou M., Krien Y., Chtioui T., Benmohammadi A. 2024. Risk Assessment of Marine Flooding along the Agadir and Taghazout Coasts (Moroccan Atlantic). *Journal of Coastal Research*, 40, 1: 179–192.

Aouiche I., Daoudi L., Anthony E.J., Sedrati M., Ziane E., Harti A., Dussouillez P. 2016. Anthropogenic effects on shoreface and shoreline changes. Input from a multi-method analysis, Agadir Bay, Morocco. *Geomorphology,* 254: 16–31.

Appeaning Addo K., Walkden M., Mills J. 2008. Detection, measurement and prediction of shoreline recession in Accra, Ghana. *ISPRS Journal of Photogrammetry and Remote Sensing*, 63: 543–558.

Armaroli C., Ciavola P., Balouin Y., Gatti M. 2004. An integrated study of shoreline variability using GIS and ARGUS Techniques. *Journal of Coastal Research,* 39: 473–477.

Atiki N., Tnourji H., Nmiss M., Ouammou A. 2021. Dynamique des vents et leurs implication dans la répartition des dunes dans la plaine de Souss Massa (centre ouest du Maroc). Publication de la Faculté des Lettres et des Sciences Humaines-Oujda: 103–109.

Barrada M. 1996. *Evolution morphologique littoral des Chtouka Ouest depuis l'ouljien*. Thèse de doctorat (N.R), Université Nancy II: 232.

Bird E.C.F. 2000. *Coastal geomorphology: An introduction*. Chichester: John Wiley & Sons.

Boak E.H., Turner I.L. 2005. Shoreline definition and detection: A review. *Journal of Coastal Research,* 21, 4: 688–703.

Bourhili A., El Khalidi K., Minoubi A., Maanan M., Zourarah B., 2023. Periodical Morphodynamic Changes of Sand Movements at El Jadida Beach. *Ecological Engineering & Environmental Technology*, 24, 4: 15–26.

Carter R.W.G. 1988. *Coastal environments: an introduction to the physical, ecological, and cultural systems of coastlines*. Academic Press, London.

Castelle B., Bonneton P., Sénéchal N., Dupuis H. 2007. Double bar beach dynamics on the high-energy meso-macrotidal French Aquitanian coast: A review. *Marine Geology*, 245, 1–4: 141–159.

Castelle B., Bujan S., Ferreira S., Dodet G. 2017. Foredune morphological changes and beach recovery from the extreme 2013/2014 winter at a high-energy sandy coast. *Marine Geology*, 385: 41–55.

Clarke K.C. 1986. Advances in geographic information systems. *Computers, Environment and Urban Systems,* 10, 3: 175–18.

Cohen O. 2014. Profiler 3.1 XL, un logiciel gratuit pour la construction et l'analyse de profils topographiques dans Microsoft Excel©. *XIII`emes Journ´ees Nationales Génie Cotier – Génie Civil*: 557–564.

Crowell M., Leatherman S.P., Buckley M.K. 1991. Historical Shoreline Change: Error Analysis and Mapping Accuracy. *Journal of Coastal Research*, 7, 3: 839–852.

Darling J.M. 1964. Seasonal changes in beaches of the North Atlantic coast of the United States. *Coastal Engineering Proceedings*, 9: 236–248.

Delgado-Fernandez I. 2011. Meso-scale modelling of aeolian sediment input to coastal dunes. *Geomorphology*, 130, 3–4: 230–243.

Dolan R., Fenster M.S., Holme S.J. 1991. Temporal Analysis of shoreline recession and accretion. *Journal of Coastal Research*, 7, 3: 723–744.

Fox W., Davis R. 1978. Seasonal variation in beach erosion and sedimentation on the Oregon coast. *Geological Society of America Bulletin*, 89: 1541–1549.

Golden Software, Inc. 2010. *Surfer Version 10 [Computer software]*. Golden, Colorado, USA.

Gopinath G., Seralathan P. 2005. Rapid erosion of the coast of Sagar island, West Bengal – India. *Environment Earth Science*: 48, 8: 1058–1067.

Hapke C., Reid D., Richmond B., Ruggiero P., List J. 2006. National Assessment of shoreline change. Part 3 Historical shoreline change and associated coastal land loss along sandy shorelines of the California coast. *US Geological Survey Open-file Report*: 72.

Hesp P.A. 2013. Conceptual models of the evolution of transgressive dune field systems. *Geomorphology*, 199: 138–149.

Himmelstoss E.A., Henderson R.E., Kratzmann M.G., Farris A.S. 2018. Digital Shoreline Analysis System (DSAS) version 5.0 user guide. *U.S. Geological Survey Open-File Report,* 2018–1179.

Houser C. 2009. Synchronization of transport and supply in beach-dune interaction. *Progress in Physical Geography*, 33, 6: 733–746.

Jabbar M. 2016. *Dynamiques morpho-sédimentaires des avant-plages et impacts sur les stocks sableux. Vers une meilleure stratégie de gestion des risques côtiers*. Thèse de doctorat, Université de Bretagne Occidentale.

Jonah F.E., Boateng I., Osman A., Shimba M.J., Mensah E.A., Adu-Boahen K., Chuku E.O., Effah E. 2016. Shoreline change analysis using end point rate and net shoreline movement statistics: An application to Elmina, Cape Coast and Moree section of Ghana's coast. *Regional Studies in Marine Science*, 7: 19–31.

Kennedy D.M. 2014. The rock coast of Australia. [in:] D.M. Kennedy, W.J. Stephenson, L.A. Naylor (eds) *Rock Coast Geomorphology: A Global Synthesis*. Geological Society. London, Memoirs, 40: 235–245.

Kılar H. 2023. Shoreline change assessment using DSAS technique: A case study on the coast of Meriç Delta (NW Türkiye). *Regional Studies in Marine Science*, 57: 102737.

Lharti S., Florb G., El kasmi S., Flor-Blanco G., El Janati M., Marcelli M., Piazzolla D., Scanu S., Della Venturae G., Boukili B., El Moutaoukkil N. 2024. Multi-decadal evolution of the Moroccan Atlantic shoreline: A case study from the Essaouira coastal sector. *Journal of African Earth Science*, 212: 1–24.

Luijendijk A., Hagenaars G., Ranasinghe R., Baart F., Donchyts G., Aarninkhof S. 2018. The state of the world's beaches. *Scientific Reports,* 8, 1: 1–11.

Mansoum M. 1994. *La baie d'Agadir impacts des aménagements sur l'évolution géomorphologique du littoral.* Thèse de doctorat, Université de Bretagne Occidentale: 349.

Masselink G., Austin M., Tinker J., O'Hare T., Russell P. 2006. Cross-shore sediment transport and morphological response on a macrotidal beach with intertidal bar morphology, Truc Vert, France. *Marine Geology,* 251, 3–4: 141–151.

Masselink G., Scott T., Poate T., Russell P., Davidson M. 2016. The extreme 2013/2014 winter storms: Hydrodynamic forcing and coastal response along the southwest coast of England. *Earth Surface Processes and Landforms*, 41, 3: 378–391.

Moore L.J. 2000. Shoreline mapping techniques. *Journal of Coastal Research,* 16, 1: 111–124.

Moore L.J. Ruggiero P., List J.H. 2006. Comparing mean high water and high-water line shorelines: should proxy-datum

offsets be incorporated into shoreline change analysis? *Journal of Coastal Research*, 22, 4: 894–905.

Morton R., Miller T., Moore L. 2004. Historical shoreline changes and associated land loss along the U.S. Gulf of Mexico. *U.S. Geological Survey. Open-file Report*: 42.

Nait-Si H., Ouammou A., Nmiss M. 2022. Apport du SIG dans l'analyse physique et hydrographique dans un bassin versant anti-atlasique. Cas du bassin versant de l'oued Adoudou. *Publication de la Faculté des Lettres et des Sciences Humaines-Oujda*: 53–58.

Naji E., Aberkan M., Saadane A., Nmiss M. 2025. Erosion and shoreline retreat indicators in the Rabat-Salé littoral and their impact on coastal planning. *Journal of African Earth Sciences*, 223: 1–12.

Naylor L.A., Stephenson W.J. Trenhaile A.S. 2010. Rock coast geomorphology: Recent advances and future research directions. *Geomorphology*, 114: 3-11.

Nicholls R.J., Cazenave A. 2010. Sea-level rise and its impact on coastal zones. *Science,* 328, 5985: 1517–1520.

Nmiss M., Amyay M., Atiki N., Tnourji H. 2021a. The morphological consequence of the storme of 1 march 2018 on a highly anthropized beach: the case of Agadir bay. *Publication de la Faculté des Lettres et des Sciences Humaines de Oujda*: 27–32.

Nmiss M. 2023*. Morphologie et dynamique actuelle du littoral atlantique marocain entre oued Massa et oued Souss*. [Thèse de doctorat, Université Sidi Mohamed Ben Abdellah-Fès].

Nmiss M., Amyay M., Atiki N., Ouammou A., Benbih M., Nait-Si H. 2025a. Seasonal morphological changes and grain size distribution mapping on the Massa beaches using topographic survey and GIS. *International Journal of Engineering and Geosciences,* 10, 2: 272–289.

Nmiss M., Amyay M., Atiki N., Ouammou A., Benbih M., Nait-Si H., Yazami Ztait M., Naji, E. 2025b. Shoreline Changes at the Souss and Massa rivers mouths, Morocco: A five decades analysis (1970-2024). *International Journal of Engineering and Geosciences*, 10, 3: 456–476.

Nmiss M., Amyay M., Ouammou A. 2021b. Dynamique du trait de côte d'une plage peu anthropisée cas de la plage Sidi Ouassai, Massa (Maroc Atlantique). *Publication de la Faculté des Lettres et des Sciences Humaines-Oujda*: 249–256.

Nmiss M., Anthony E., Amyay M., Ouammou A. 2022. Multi-decadal shoreline change, inherited coastal morphology and sediment supply in the Souss-Massa littoral cell (Morocco), and a prognosis with sea-level rise. *Journal of African Earth Science*, 196: 1–12.

Pardo-Pascual J.E., Almonacid-Caballer J., Ruiz L.A., Palomar-Vázquez J. 2012. Automatic extraction of shorelines from Landsat TM and ETM+ multi-temporal images with subpixel precision. *Remote Sensing of Environment*, 123: 1–11.

Paskof R., Clus-Auby C. 2007. L'érosion des plages les causes, les remèdes. *Publication de l'Institut Océanographique*, Paris: 185.

Poate T., Masselink G., Russell P., Austin M. 2014. Morphodynamic variability of high-energy macrotidal beaches, Cornwall, UK. *Marine Geology*, 350: 97–111.

PORTUS. Puertos del Estado (Spain). PORTUS Coastal Observatory Database. Available at: https://portus.puertos.es.

Robin M. 2005. Télédétection et modélisation du trait de côte et de sa cinématique. Le littoral regard et pratiques et savoirs, Éditions Rue d'Ulm, Presses Universitaires de l'Ecole Normale Supérieure, Paris : 87–115.

Salman A., Lombardo S., Doody P. 2004. Living with coastal erosion in Europe: sediment and space for sustainability. Part II Maps and statistics., Brussels. *Report Directorate General of Environment*, European Commission: 25.

Stafford D.B., Langfelder J. 1971. Air photo survey of coastal erosion, *Photogrammetric Engineering,* 37: 565–575.

Telkin M. 2004. Un type original de dunes embryonnaires sur la plage macrotidale du fort vert (Pas-de-Calais, France). *Bulletin de l'Association des Géographes Français*, 81, 3: 418–426.

Temitope D., Oyedotun, T. 2014. Shoreline Geometry: DSAS as a tool for historical trend analysis. *Geomorphological Techniques,* 3: 1–12.

Theiler E.R., Danforth W.W. 1994. Historical shoreline mapping (I): improving techniques and reducing positioning errors. *Journal of Coastal Research,* 10, 3: 549–563.

Thomas Y.F., Diaw A.T. 1997. Suivi (1984-1993) de la rupture de la fèche de Sangomar, estuaire du Saloum, Sénégal. *Photo-Interprétation*, 3: 199-204.

USGS EarthExplorer. U.S. Geological Survey (USGS). EarthExplorer: Online data search and download platform for remote sensing data. Available at https://earthexplorer.usgs.gov/.

Uścinowicz G., Uścinowicz Sz., Szarafin T. 2025. Short-term coastal dynamics and implications for energy infrastructure safety: insights from the Baltic Sea coast, *Geological Quarterly*, 69: 34.

Vousdoukas M.I., Almeida L.P., Ferreira Ó. 2012. Beach erosion and recovery during consecutive storms at a steep-sloping, meso-tidal beach. *Earth Surface Processes and Landforms,* 37, 6: 583–593.

Vousdoukas M.I., Ranasinghe R., Mentaschi L., Plomaritis T.A., Stive M.J.F., Feyen L. 2020. Sandy coastlines under threat of erosion. *Nature Climate Change*, 10, 3: 260–263.

Zhang K., Douglas B.C., Leatherman S.P. 2004. Global warming and coastal erosion. *Climatic Change*, 64, 1–2: 41–58.